Liebson, I., E. G. Holcomb, A. G. Cacoso, and J. J. Jacmic, "Rate of Flow and Mechanics of Bubble Formation from Single Submerged Orifices," *ibid.*, 2, 296 (1956).

Morton, B. R., "Modeling Fire Plumes," Tenth Symp. (Intern.) on Combustion, pp. 973-982, The Combustion Institute, Pittsburgh, Pa., (1965).

Murgai, M. P., and H. W. Emmons, "Natural Convection Above Fires," *J. Fluid Mech.*, 8, 611 (1960).

Ricou, F. P., and D. B. Spalding, "Measurements of Entrainment of Axisymmetrical Turbulent Jets," *ibid.*, 11, 21 (1961).

Stanford, L. E., and C. C. Webster, "Energy Suppression and Fission Product Transport in Pressure-Suppression Pools," Oak Ridge Nat. Lab. Report, ORNL-TM-3448 (1972).

Weimer, J. C., M.S. thesis, Penn. State Univ., University Park (1972).

Manuscript received September 11, 1972; revision received December 8, 1972; paper accepted December 11, 1972.

Photopolymerization of Acrylamide in an Annular Flow Reactor

Rates of homogeneous polymerization of aqueous solutions of acrylamide were measured in an annular flow reactor at 35°C. By independent determinations of the quantum yield for the initiation step and the light intensity, it was possible to identify reaction orders and to calculate ratios of rate constants for the polymerization process.

An empirical kinetics model, based upon producing activated molecules solely from initiator ($K_2S_2O_8$), best fit the data. According to this model the rate is 3/2 order in monomer concentration, 1/2 order in initiator, and proportional to the 1/2 power of the intensity of absorbed radiation. The effect of monomer concentration on the induction period and the 3/2 order with respect to monomer indicate a complex initiation process.

DAN SANDRU
and
J. M. SMITH

Department of Chemical Engineering
University of California
Davis, California

SCOPE

Kinetic studies of homogeneous photopolymerization in batch systems have a long history (Bagdasar'yan, 1968, 1944, 1947, 1948, 1949; Bamford, 1949; Bevington, 1961; Flory, 1953; Hamm, 1967; Huysor, 1970; Mark and Raff, 1961; Marvel and Levesque, 1939; Marvell and Riddle, 1940; Newkirk, 1946; Taylor and Vernon, 1930). The objectives in these investigations were to determine the effect of concentrations and light intensity on the rate. Only rarely were numerical values obtained for the kinetic constants. From an applied viewpoint it is important to be able to use kinetic data to predict the performance of continuous flow reactors. For this purpose it is necessary to have a numerical rate equation and also a design procedure to account for the variations in rate with location in the reactor. This engineering aspect of photopolymerization has not been treated in the literature to our knowledge, except in a recent work by Jain, Graessley, and Dranoff (1970) on styrene polymerization in dilute solutions.

The objective of this work was to measure rates quantitatively for a typical system—the polymerization of acrylamide in an annular flow differential reactor. Acrylamide was chosen since it represents a typical monomer which forms water-soluble polymer and since some numerical rate information obtained in a batch system (Suen et al., 1958) is available. The data were used to test models for the kinetics of the polymerization process, particularly to determine the order of the rate with respect to monomer and initiator concentrations and with respect to light intensity.

CONCLUSIONS AND SIGNIFICANCE

The practicality of an experimental method for measuring photopolymerization rates in a flow reactor has been demonstrated by studying the homogeneous polymerization of acrylamide with a polychromatic radiation source. It was shown that the quantum yield for the initiation step can be estimated by first operating the annular reactor as a batch-recycle unit during the induction period. In the subsequent part of a run, operation was changed to a once-through differential basis for which rates of polymerization could be measured.

It was shown further that the rate data, combined with independent measurements of light intensity and of quantum yield for the initiation step, could be used to evaluate various models of polymerization kinetics. In particular the order of the overall reaction with respect to concentrations and light intensity could be established. For our acrylamide study the 1.5 order for monomer concentration indicated an interaction effect, such as complex formation, or cage effect, between monomer and activated initiator molecules. Also numerical values of rate-constant ratios could be evaluated based upon certain assumptions, par-

ticularly concerning the intensity distribution in the reactor. The experimental method and type of analysis should be useful for obtaining rate equations suitable for photoreactor design.

The measured rate in a photoreactor, even for so-called "differential operation with respect to concentrations," is an average value. This is because the intensity varies with position. An annular reactor arrangement (Figure 2) with the photolamp located along the central axis was used in our work. Jain, Graessley, and Dranoff (1970) derived an expression for the intensity as a function of position in the annulus considering radiation emanating in all directions from the lamp taken as a line source. This formulation is particularly useful when the entire lamp and reactor are visible to each other; for at the ends of the reactor deviations from a radial radiation model are serious. In the arrangement shown in Figure 2, brass sleeves were inserted in the space between the lamp and reactor to reduce nonradial radiation. Hence, the simpler radial model was used. Errors introduced by this simplification should not influence significantly the effect of variables on the rate but would affect its numerical value. By using the same radiation model for both the actinometer runs used to calculate the absolute intensity and the polymerization runs, such errors are reduced.

With the assumptions of no reflection and refraction and using the radial model, the application of Lambert's law to the geometry of Figure 2 gives

$$I_{r,\lambda} = \frac{\eta R}{r} I_{w,\lambda} \exp\left[-\mu_\lambda (r - \eta R)\right] \tag{1}$$

$I_{w,\lambda}$ is the intensity at the inner radius ηR of the annulus when there is no filter solution in the jacket. Equation (1) also neglects absorption by air, quartz, and distilled water; these absorptivities are very low in the near-UV region where the lamp provides significant radiation.

RATE MODELS

A generally accepted mechanism of homogeneous polymerization has not been established. Various researchers, for example, Denbigh (1947) and Tudos (1964, 1965), have developed rate equations applicable in restricted domains. A well-known relation, based upon activation of initiator molecules by radiation followed by free-radical polymerization reactions, is

$$\Omega = \frac{k_i^{1/2}\, k_p}{k_t^{1/2}} [In]^{1/2} [M] \tag{2}$$

In the derivation of Equation (2), the propagation and termination rate constants are taken as constant, regardless of the number of monomer units in the free radicals. Also the stationary state assumption is applied to activated initiator molecules and to free radicals of polymer, and the termination processes are limited to combination and disproportionation of free radicals into stable polymer.

In many cases the effect of monomer concentration is more complex than the first-order dependency given by Equation (2). In these instances the order is usually greater than unity. Various theories have been advanced by way of explanation: the cage effect, Matheson (1945), Noyes (1955); complex formation, Kamenskaya and Medevedev (1940), Mark and Josefowitz (1945), Schulz and Husemann (1938); termination by primary radicals, Bamford et al. (1959), Chapiro et al. (1955), Goppalan and Santappa (1963); and a solvent retardation effect, Burnett and Loan (1959). None of these explanations are accepted as entirely satisfactory (Jenkins, 1958).

In our experiments the effect of monomer concentration on the rate was greater than first order and the induction period was dependent upon $[M]$. This suggests that monomer is somehow involved in the initiation step. Of various possibilities, the most successful theoretical equation is based upon the concept that monomer, in the presence of initiator, could also form activated species capable of causing polymerization. The sequence of steps can be represented as follows:

$$\left.\begin{aligned} In &\xrightarrow{k_{iIn}} 2X^\cdot \\ \mathrm{M} &\xrightarrow{k_{iM}} \mathrm{X}^\cdot \end{aligned}\right\} \text{initiation} \tag{3}$$

$$\left.\begin{aligned} X^\cdot + M &\xrightarrow{k_p} R_1^\cdot \\ R_1^\cdot + M &\xrightarrow{k_p} R_2^\cdot \end{aligned}\right\} \text{propagation} \tag{4}$$

$$R_n^\cdot + R_m^\cdot \xrightarrow{k_t} R_{n+m} \quad \text{termination} \tag{5}$$

Employing the same assumptions as used in deriving Equation (2), the total concentration of free-radical polymer is

$$\sum_{i=1}^{n} [R_i^\cdot] = \frac{[2k_{iIn}\,[In] + k_{iM}[M]]^{1/2}}{(2k_t)^{1/2}} \tag{6}$$

If the numerator of Equation (6) is expanded using the binomial expansion and all terms after the second are assumed to be negligible,

$$\sum_{i=1}^{n} [R_i^\cdot] = \frac{1}{(2k_t)^{1/2}} \left\{ \sqrt{2}\, k_{iIn}{}^{1/2}\, [In]^{1/2} + \frac{k_{iM}[M]}{(2)^{3/2}\, k_{iIn}{}^{1/2}\, [In]^{1/2}} \right\} \tag{7}$$

Then the rate of production of polymer, given by the sum of the propagation reactions, becomes

$$\Omega(r) = k_p[M] \sum_{i=1}^{n} [R_i^\cdot] = \frac{k_p}{(2k_t)^{1/2}} [M] \left\{ \sqrt{2}\, k_{iIn}{}^{1/2}\, [In]^{1/2} + \frac{k_{iM}[M]}{2^{3/2}\, k_{iM}{}^{1/2}\, [In]^{1/2}} \right\} \tag{8}$$

Equation (8) exhibits a net effect of $[M]$ greater than first order, as does the experimental data. However, it will be seen that the values of the rate-constant ratio $k_p/k_t^{1/2}$ determined from the experimental results, are not as consistent as those from the empirical expression

$$\Omega(r) = k_i^{1/2} \left(\frac{k_p}{k_t^{1/2}}\right)_E [In]^{1/2} [M]^\beta \tag{9}$$

where the order of $[M]$ is a parameter to be evaluated from the measured rates and the empirical nature of the rate-constant ratio is denoted with the subscript E.

Before the local rate can be compared with the data, the equations for $\Omega(r)$ must be expressed in terms of intensity and then integrated over the reactor volume. This leads to complicated-appearing equations, but these complications are due to the light-distribution function and do not significantly disturb order of the rate with respect to concentrations and intensity. For a photochemical initiation step the rate constant is, assuming that the rate is proportional to the light absorbed,

$$k_i = \sum_{\lambda} \phi_\lambda \alpha_\lambda I_{r,\lambda} \tag{10}$$

where ϕ is the quantum yield and $I_{r,\lambda}$ the local intensity. The absorptivity α is related by Beers' law to the attenuation coefficient and the concentration of absorbing species by the equation

$$\mu_\lambda = \alpha_\lambda [C] \tag{11}$$

The local intensity is given by Equation (1) and this can be expressed, in terms of the total intensity $I_{b,t}$ (at ηR) and the spectral energy distribution of the lamp, by

$$I_{w,\lambda} = I_{b,t} \frac{F_\lambda}{F_t} T_\lambda \tag{12}$$

Combining Equations (1) and (12), and substituting the resulting expression for $I_{r,\lambda}$ and Equation (11), in Equation (8) leads to

$$\Omega(r) = \left(\frac{k_p}{k_t^{1/2}}\right)\left(\frac{\eta R}{r}\right)^{1/2} \frac{[M] I_{b,t}^{1/2}}{2^{1/2}} \left\{ 2^{1/2}[In]^{1/2} \left[\sum_{\lambda} T_\lambda \frac{F_\lambda}{F_t} \phi_{\lambda,In}\, \alpha_{\lambda,In} \exp\left[-\mu_{\lambda,In}(r-\eta R)\right] \right]^{1/2} + \frac{1}{2^{3/2}} \frac{[M]}{[In]^{1/2}} \frac{\sum_{\lambda} T_\lambda \frac{F_\lambda}{F_t} \phi_{\lambda,M}\, \alpha_{\lambda,M} \exp\left[-\mu_{\lambda,M}(r-\eta R)\right]}{\left[\sum_{\lambda} T_\lambda \frac{F_\lambda}{F_t} \phi_{\lambda,In}\, \alpha_{\lambda,In} \exp\left[-\mu_{\lambda,In}(r-\eta R)\right]\right]^{1/2}} \right\} \tag{13}$$

Equation (13) gives the local rate in terms of r. For differential-reactor operation (with respect to concentration) the only variable in the reactor volume is r. Since a radial model for intensity is used, integration over the reactor length is not necessary. Integrating with respect to $2\pi r dr$ and dividing by the cross-sectional area gives average rate $\overline{\Omega}$. If average quantum yields for the region of the polychromatic lamp are used instead of $\phi_{\lambda,In}$ and $\phi_{\lambda,M}$, the result is

$$\overline{\Omega} = 2^{1/2}\left(\frac{k_p}{k_t^{1/2}}\right) \frac{\eta^{1/2}[M]}{R^{3/2}(1-\eta^2)} I_{b,t}^{1/2} \left\{ 2^{1/2}[In]^{1/2}\phi_{In}^{1/2} \int_{\eta R}^{R} \left[\sum_{\lambda} T_\lambda \frac{F_\lambda}{F_t} \alpha_{\lambda,In} \exp\left[-{}_{\lambda,In}(r-\eta R)\right] \right]^{1/2} r^{1/2} dr + \frac{1}{2^{3/2}} \frac{[M]\,\phi_M}{[In]^{1/2}\,\phi_{In}^{1/2}} \int_{\eta R}^{R} \frac{\sum_{\lambda} T_\lambda \frac{F_\lambda}{F_t} \alpha_{\lambda,M} \exp\left[-\mu_{\lambda,M}(r-\eta R)\right]}{\left[\sum_{\lambda} T_\lambda \frac{F_\lambda}{F_t} \alpha_{\lambda,In} \exp\left[-\mu_{\lambda,In}(r-\eta R)\right]\right]^{1/2}} \right\} r^{1/2} dr \tag{14}$$

The analogous expression for $\overline{\Omega}$ based upon Equation (9) is

$$\overline{\Omega} = \frac{2\eta^{1/2}}{R^{3/2}(1-\eta^2)} \left(\frac{k_p}{k_t^{1/2}}\right)_E [In]^{1/2} [M]^{\beta} I_{b,t}^{1/2}\, \phi_{In}^{1/2} \int_{\eta R}^{R} \left[\sum_{\lambda} T_\lambda \frac{F_\lambda}{F_t} \alpha_{\lambda,In} \exp\left[-\mu_{\lambda,In}(r-\eta R)\right] \right]^{1/2} r^{1/2} dr \tag{15}$$

Equation (14), while appearing complex because of the summations and integrals, clearly suggests an order with respect to $[M]$ of more than unity, one-half order in intensity, and a less than one-half net order with respect to $[In]$. The orders suggested by Equations (14) and (15) are the same as those indicated by the local rates [Equations (8) and (10) or (9) and (10)]. The integrals in Equations (14) and (15) can be evaluated numerically by first measuring the attenuation coefficients in a spectrophotometer as a function of wave length and concentration of monomer or sensitizer (initiator). The absorptivities can be obtained from μ using Equation (11). The measured transmittance T_λ of the filter solutions and the lamp manufacturer's data for F_λ and F_t give $(F_\lambda/F_t)T_\lambda$. The experimentally determined induction periods establish the quantum yield ϕ_{In} in Equation (15) and the sum of ϕ_{In} and ϕ_M in Equation (14). There remains one free parameter, in addition to $k_p/k_t^{1/2}$, in each equation. This is the exponent β on $[M]$ in Equation (15) and the ratio of quantum yields in Equation (14). The test of the suitability of the equations is how well they predict the orders of monomer and initiator concentrations and light intensity on the rate, and how well experimental and calculated rates agree with a single value of $k_p/k_t^{1/2}$. The program of experimental measurements was designed to provide such tests.

EXPERIMENT

Exploratory runs were made in an annular-type, batch reactor of 400 cm^3 irradiated volume. A medium-pressure mercury lamp (Hanovia (679A, 400 watt) was inserted in a quartz well which was enclosed in a quartz cooling jacket and the annular reactor. The output of the lamp from 2224Å to 3660Å is available.* Only within this wave length range is there significant absorption by initiator or monomer. From the exploratory data it was determined that potassium persulfate was a suitable initiator, and that at a temperature in the range 35 to 40°C photopolymerization was significant and dark reaction negligible. Also it was established that conditions for most accurate differential rate measurements were conversions from 5 to 15%, with monomer and initiator concentrations from 0.05 to 0.5 g moles/liter and 2.6×10^{-4} to 2.1×10^{-3} g moles/liter, respectively. These concentration ranges are close to practical levels.

Data for accurate rate determination were obtained in the apparatus shown in Figure 1, which could be operated either as a differential-flow or batch-recycle reactor. The seven-liter reservoir (2) served as a feed tank for differential-reactor operation and as a reservoir in the batch-recycle mode. Oxygen

---

* Additional material has been deposited as Document No. 02092 with the National Auxiliary Publications Service (NAPS), c/o Microfiche Publications, 305 E. 46th St., N. Y., N. Y. 10017 and can be obtained for $1.50 for microfiche and $6.00 for photocopies.

could be added through cylinder (8) or removed by bubbling helium from (7) into the reservoir. Dissolved gas concentrations were measured by feeding liquid samples from tank (19) to a stripping column (10), whose gaseous product was analyzed in chromatograph (9). Samples were taken for polymer determination at the entrance (12a) and exit (12b) of the reactor for the differential-reactor runs, and from sample line (11) during batch-recycle operation.

The annular reactor and inner jackets of optically clear quartz are shown with dimensions in Figure 2. The feed was introduced into the annulus in four equal streams spaced at 90° angles in order to minimize rotational flow. In addition, a calming length of 500 mm of annulus was provided upstream from the irradiated section. The length of this section was adjusted to 100 mm using thin brass sleeves around the lamp and jacket as shown in Figure 2. The sleeves also provided a central section of near-uniform radiation. Downstream was a similar calming section of 300 mm length, after which the effluent left the system in four streams spaced at 90° angles. The volume of the irradiated section was 283 cm^3, and this value was used in calculating the reaction rate. Because of nonradial radiation the true reactor volume probably was somewhat larger than 238 cm^3. Temperatures in the reactor were measured with a movable iron-constantan thermocouple. Axial gradients were less than 1°C.

A high-pressure mercury (Hanovia LL 189A, 1200 watt) with the UV energy spectrum given in Table 1 was the radiation source for all quantitative rate data obtained in the flow reactor. Cooling was accomplished with air flow in the inner jacket and water or filter solution flowing in the next jacket (Figure 2).

The effect of intensity was studied by circulating solutions of $Fe\,Cl_3 \cdot 6H_2O$ through the filter-solution jacket. By adjusting the concentration of $FeCl_3$, it was possible to obtain a 30-fold variation in intensity without significant changes in spectral distribution. The transmittances of the filter solutions used are also available.[*]

In making a run, dissolved oxygen was first reduced to a low level by bubbling helium through the reservoir (2) containing the monomer-initiator solution. Next, the system was operated as a batch-recycle reactor, with a recirculation rate of 1800 cm^3/min, until a slight amount of polymer was detected in the sample from line (11). After this the lamp was extinguished for 15 minutes to allow time for destruction of all free radicals. Then the lamp was started again and the system operated as a differential reactor with flow rates of 150 to 200 cm^3/min. By estimating the time at which polymer first was produced, approximate values for the induction time T were obtained. These results are shown in Figure 3 for different light intensities as measured by $\Sigma[(F_\lambda/F_t)T_\lambda\,\alpha_{In,\lambda}]$, monomer, and initiator concentrations. The increase in T with decrease in intensity and with $[In]$ is expected, since the rate of initiation decreases. However, the effect of $[M]$ is not easily understood. It was found that polymerization does not occur with no initiator present. Hence, if activated species are formed from monomer [Equation (3)], the process must be affected also by initiator molecules.

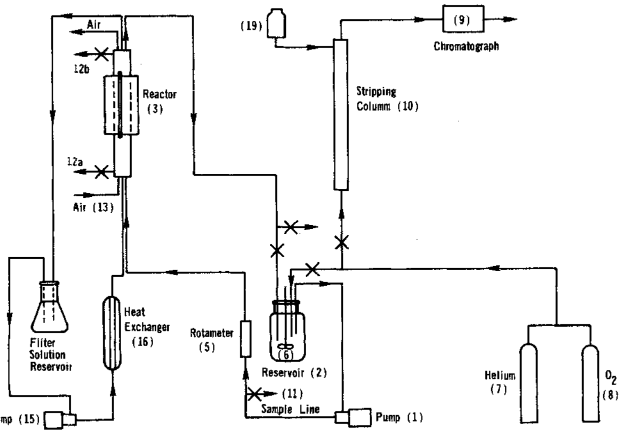

Fig. 1. Schematic diagram of flow-reactor apparatus.

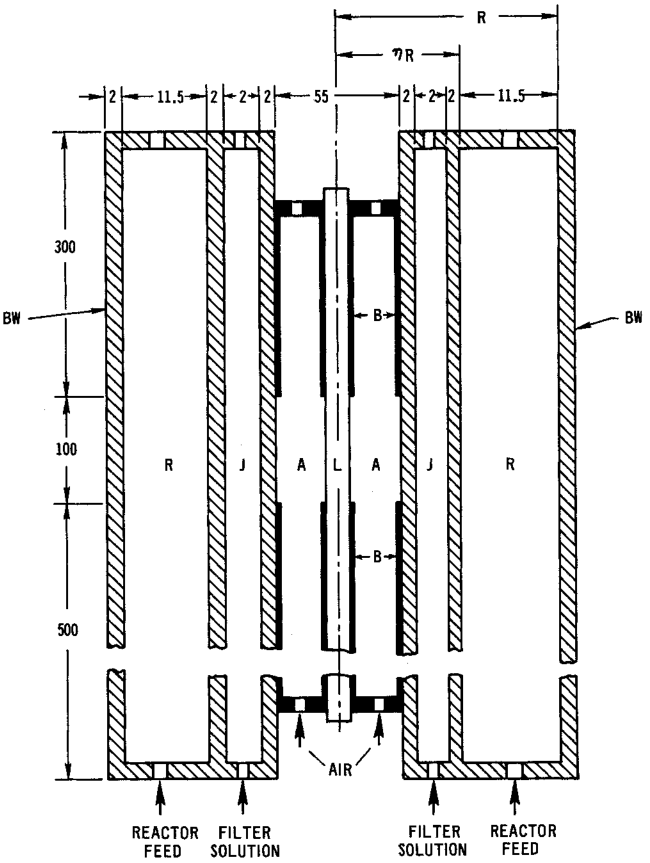

Fig. 2. Reactor layout and dimensions (mm): *R* = reactor annulus; *J* = filter solution jacket; *L* = lamp; *A* = air jacket; *BW* = blackened outer wall of reactor; *B* = brass sleeves.

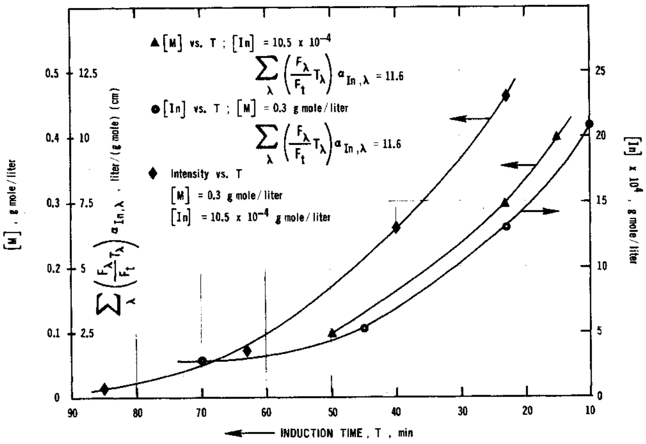

Fig. 3. Induction period data.

For both batch-recycle and differential operation, the flow was streamline in the reactor, with Reynolds' numbers from about 1 to 10. However, velocity distribution need not be considered in evaluating rates from the data since the reactor operated differentially; that is, conversions were less than 10%.

To determine polymer content, 5 cm^3 samples were taken from the system and the polymer was precipitated with 200 cm^3 of methanol. After filtration and washing with an additional 200 cm^3 of methanol, the polymer was dried at 50 to 65°C until the weight was constant. Tests with samples of commercial polymer showed a systematic error of about 3% in this method of analysis, presumably due to a small amount of polymer remaining in solution or otherwise lost. A 3% correction was added to all the analytical results. The rates calculated using these analytical results and Equation (22)

---

[*] See footnote on page 560.

were reproducible within 5%. The acrylamide (laboratory grade) used was a Matheson, Coleman and Bell product and had a melting point of 83 to 85°C. The $K_2S_2O_8$ was from Mallinckrodt Chemical Company and had a stated, minimum purity of 99%.

AUXILIARY DATA

Absorptivities

Absorption data (absorbance, A) were measured from 1900 to 3500Å at 35°C for acrylamide and potassium persulfate in a spectrophotometer. Illustrative results for specific concentrations are shown in Figure 4 where $A_\lambda = \log_{10}(1/T_\lambda)$ is plotted versus wave length. Then absorptivities were calculated from the expression

$$\alpha_\lambda = \frac{2.303\,A_\lambda}{CL} \tag{16}$$

and are available.* Absorptivities of monomer are higher than those for initiator except at wave lengths greater than about 2800Å. While α_λ values are low for both substances at $\lambda > 2800$Å, much of the energy output of the lamp is at these longer wave lengths.

Intensity Measurements

The radiation intensity at the reactor wall ($r = \eta R$) was determined by measuring the extent of oxalic acid decomposition when aqueous solutions of oxalic acid and uranyl sulfate flowed through the reactor in batch-recycle operation. The rate was calculated from the slope of the concentration versus time curve according to the equation

$$\overline{\Omega}_{Ox} = \frac{-V_s}{V_R}\,\frac{d[\mathrm{Ox}]}{dt} \tag{17}$$

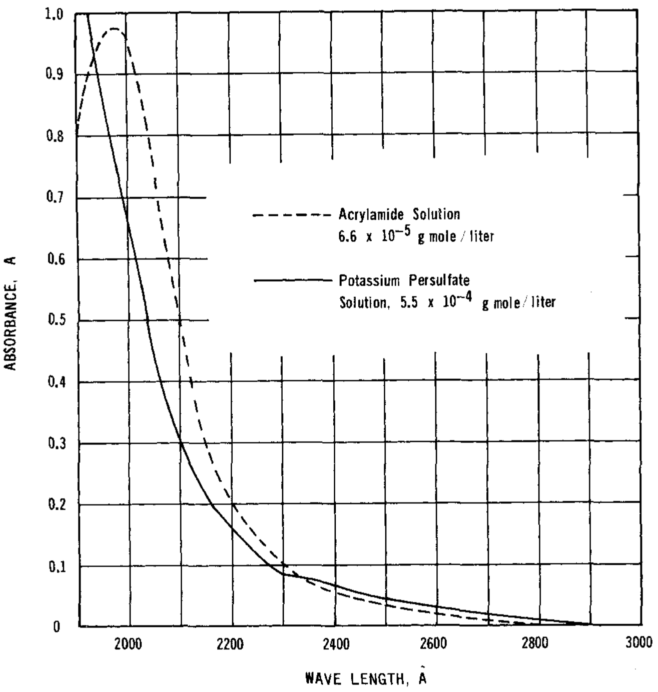

Fig. 4. Absorption data for acrylamide and initiator at 35°C.

Since the uranyl ion sensitized reaction is zero order in oxalic acid concentration, the [Ox] versus t curve was linear (that is, was constant) after steady state was achieved.

Using the radial intensity profile [Equation (1)] in the local rate equation

$$\Omega(r)_{Ox,\lambda} = \phi_{Ox,\lambda}\,\mu_\lambda\,I_{r,\lambda} \tag{18}$$

the following expression can be developed for the total intensity $I_{b,t}$ at $r = \eta R$:

$$I_{b,t} = \frac{\overline{\Omega}_{Ox}}{\dfrac{2}{R}\,\dfrac{\eta}{1-\eta^2}\,\sum\limits_{\lambda} \phi_{Ox,\lambda}\,\dfrac{F_\lambda}{F_t}\,T_\lambda\{1 - \exp[-\mu_{Ox,\lambda}\,R(1-\eta)]\}} \tag{19}$$

The derivation is analogous to that used in obtaining Equation (14) and has been illustrated in detail by Cassano and Smith (1966) for a different lamp-reactor geometry. The quantum yield and attenuation coefficient are known for this actinometer reaction [Cassano and Smith (1966)], and $T_\lambda = 1.0$ since distilled water was circulated through the filter jacket. Then $I_{b,t}$ could be calculated from the measured values of $\overline{\Omega}_{Ox}$. A run made just prior to the polymerization studies gave $\overline{\Omega}_{Ox} = 2.52 \times 10^{-4}$ g mole/(liter)(sec) and $I_{b,t} = 2.04 \times 10^{-6}$ Einsteins/(cm^2)(sec). For the run after completing the polymerization data, $\overline{\Omega}_{Ox} = 2.26 \times 10^{-4}$ g mole/(liter)(sec) and $I_{b,t} = 1.82 \times 10^{-6}$ Einsteins/(cm^2)(sec). Since the new lamp may not have reached steady state output at the time of the first actinometer test, the lower value for $I_{b,t}$ was used in evaluating polymerization rate constants.

Quantum Yield of Initiation Step

The oxygen-inhibitor method Calvert and Pitts (1966) was used to establish ϕ_{In}. The method is based upon the fact that the rate of the reaction between initiator radicals $X^\cdot$ and oxygen

$$2X^\cdot + O_2 \rightarrow X_2O_2 \tag{20}$$

is much greater than

$$X^\cdot + M \rightarrow R_1^\cdot$$

or the rate of deactivation of $X^\cdot$. Then the rate of the initiation step

$$In + h\nu \rightarrow 2X^\cdot$$

can be determined by following the elimination of oxygen. Since the initiator concentration is always more than 10-fold that of the initial oxygen concentration, $[In]$ remains nearly constant. Thus the rate is nearly constant throughout the induction period.

Special runs were made by first preparing a solution of monomer and initiator saturated with oxygen. The monomer was purified of any impurities that might react with initiator radicals by solution and reprecipitation from methanol-water solutions. The rate of initiation was calculated from the batch, recycle equation

$$\overline{\Omega}_{In} = \frac{[O_2]_0\,V_s}{T\,V_R}$$

where $[O_2]_0$ and T are the measured initial concentration of dissolved oxygen and the induction time. The average value of $\overline{\Omega}_{In}$ from several runs was 3.33×10^{-5} g mole/(liter)(sec). Finally, ϕ_{exp} was obtained from an equation similar to Equation (19) except applied to the initiation reaction; that is,

---

* See footnote on page 560.

$$\phi_{\mathrm{exp}} = \frac{\bar{\Omega}_{In}}{\dfrac{2}{R}\,\dfrac{\eta}{1-\eta^2}\,I_{b,t}\,\sum\limits_{\lambda} \dfrac{F_\lambda}{F_t}\,T_\lambda \{1 - \exp\,[-\,\mu_{In,\lambda}\,R(1-\eta)]\}} \tag{21}$$

This equation gives an average value with respect to the polychromatic radiation of the lamp. As Figure 4 shows, T is a function of concentrations and intensity. Hence ϕ_{exp} also depends upon these variables. A single, average value of ϕ_{exp} was established by determining T at concentrations midway in the range studied, that is, for $[M] = 0.3$ g mole/liter and $[In] = 10.5 \times 10^{-4}$ g moles/liter and for the highest intensity, where most of the rates were measured. Using $I_{b,t}$ determined from the actinometer data, a value of $\phi_{\mathrm{exp}} = 0.154$ is obtained. Similar quantum yields using other initiators, monomers, and light intensities cover a wide numerical range. For example, Jain et al. (1970) reported values of 0.185 and 0.42 for styrene polymerization with azo-bis-isobutyro-nitrile.

The α_λ, $I_{b,t}$ and ϕ values reported here are used to evaluate the rate models, Equations (14) and (15).

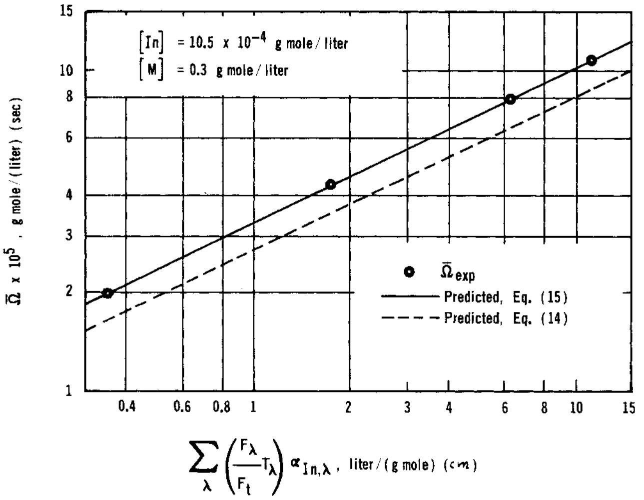

Fig. 5. Effect of intensity on polymerization rate.

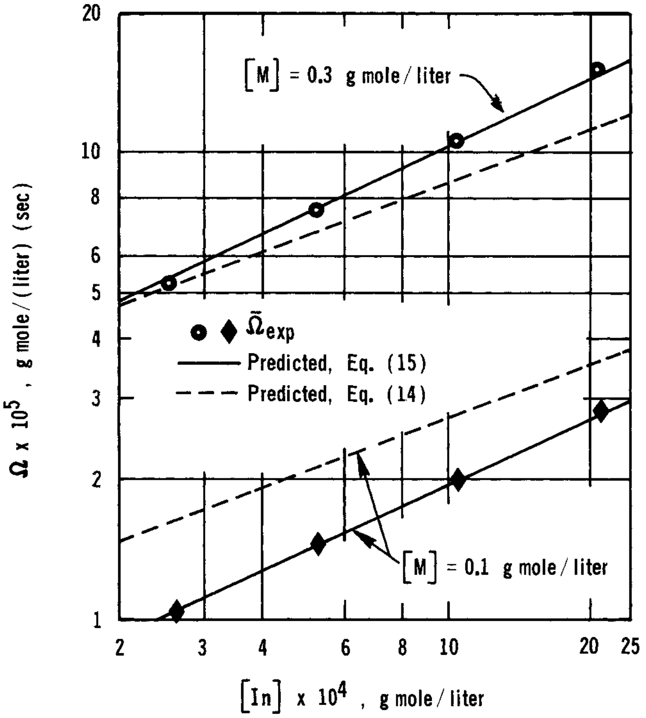

Fig. 6. Reaction rate vs. initiator concentration.

A representative sample of polymer produced in the reactor was used to determine viscosity versus polymer concentration data. The measurements were made for polymer-water solutions in a co-axial cylinder viscometer. Extrapolating the data to zero concentration gave a value of 3.2 deciliter/g for the intrinsic viscosity of the polymer solution. Using the viscosity versus molecular weight relation for acrylamide polymer (Bagdasar'yan, 1968); Fujimoto, 1967); Suen et al., 1958) an average molecular weight of 1.3×10^6 was obtained. This result is similar to values of 1 to 2×10^6 measured for polymer produced by thermal polymerization, Fujimoto (1967).

POLYMERIZATION KINETICS

Experimental polymerization rates were calculated from the differential-reactor runs using the equation

$$\bar{\Omega}_{\mathrm{exp}} = \frac{[M]_0 - [M]_p}{V_R/Q} \tag{22}$$

Data were obtained for the effect of light intensity, and initiator and monomer concentrations. For evaluating the influence of $[M]$ and $[In]$, distilled water was used in the filter-solution jacket so that the highest light intensity was obtained. The results are given in Figures 5 to 7.

The rate data in Figure 7 show a 1.5 power dependency on $[M]$ so that $\beta = 1.5$ in Equation (15). This equation is based upon the concept that only initiator molecules are activated. Hence, the measured quantum yield $\phi_{\mathrm{exp}} = 0.154$ would be equal to ϕ_{In} in Equation (15) and $\mu_{\lambda,In}$ and $\alpha_{\lambda,In}$ apply only to initiator. Then all quantities on

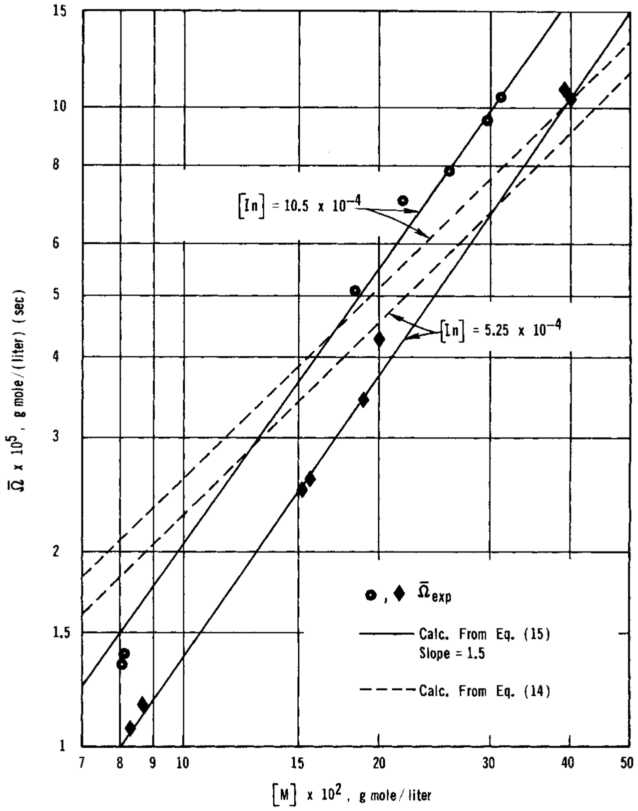

Fig. 7. Effect of monomer concentration on the rate.

TABLE 1. POLYMERIZATION RATE RESULTS

Initiator conc., $[In] \times 10^4$ g mole/liter	Monomer conc., $[M]$ g mole/liter	Exp. rate $\overline{\Omega}_{\exp} \times 10^5$ g mole/(liter)(s)	$\sum_\lambda \frac{F_\lambda}{F_t} T_\lambda \alpha_{\lambda, In}$ liter/(g mole)(cm)	$(k_p/k_t^{1/2})_E$, Equation (15) liter/(g mole)(s)$^{1/2}$	$k_p/k_t^{1/2}$, Equation (14) [liter/(g mole)(s)]$^{1/2}$
2.62	0.10	1.05	11.6	2.92	0.0575
5.25	0.10	1.50	11.6	3.00	0.0647
10.5	0.10	2.08	11.6	3.02	0.0682
21.0	0.10	2.88	11.6	3.03	0.0703
2.62	0.30	5.34	11.6	2.84	0.0950
5.25	0.30	7.55	11.6	2.88	0.105
10.5	0.30	10.5	11.6	3.18	0.111
21.0	0.30	15.1	11.6	3.01	0.120
5.25	0.082	1.07	11.6	2.92	0.0472
5.25	0.087	1.21	11.6	3.01	0.0500
5.25	0.151	2.52	11.6	2.79	0.0605
5.25	0.154	2.62	11.6	2.78	0.0590
5.25	0.186	3.46	11.6	2.89	0.0664
5.25	0.200	4.31	11.6	3.11	0.0780
5.25	0.391	11.5	11.6	3.04	0.107
5.25	0.395	10.8	11.6	2.83	0.0992
10.5	0.080	1.40	11.6	2.83	0.0579
10.5	0.081	1.47	11.6	2.92	0.0597
10.5	0.184	5.16	11.6	3.12	0.0906
10.5	0.218	7.03	11.6	3.34	0.109
10.5	0.247	7.90	11.6	2.97	0.103
10.5	0.300	10.5	11.6	2.97	0.112
10.5	0.312	11.3	11.6	3.00	0.114
10.5	0.359	13.1	11.6	2.83	0.116
10.5	0.378	14.4	11.6	2.86	0.120
10.5	0.300	2.07	0.352	3.00	0.103
10.5	0.300	4.38	1.78	2.99	0.110
10.5	0.300	7.91	6.42	3.07	0.109
10.5	0.300	10.5	11.6	2.99	0.106
			Average	2.97	0.088

the right side of the equation are known except $(k_p/k_t^{1/2})_E$. The measured rates were used to evaluate this ratio of rate constants and the values are given in Table 1. Results are shown for the runs with variable light intensity even though $\phi_{\exp} = 0.154$ is not as appropriate for these data points. The average value of the ratio is 2.97, and there appears to be no trend in the deviations, which fall within ± 7%, except for one value of 3.34. Using the average value, rates were calculated from Equation (15) and are shown as solid lines in Figures 5 to 7. Figures 5 and 6 demonstrate that the data follow closely the ½ power effect of light intensity and initiator concentration, suggested by Equation (15). Also the predicted rates, according to the 1.5 order of $[M]$, agree reasonably well with the data in Figure 7. Other data in the literature have indicated β to be greater than unity. Fujimoto (1967) found a 1.5 order using riboflavin as initiator, and a range of $\beta = 1$ to 2.5 was observed by Suen et al. (1958) using a chlorate-sulfite redox system as initiator. A few runs were also made using azo-bis-isobutyro-nitrile as initiator. Due to the low solubility of this substance in water, a concentration of only 1.1×10^{-5} g mole/liter could be used. Though the polymerization rates were low, a 1.5 order of rate with respect to $[M]$ was also found.

In addition, Table 1 gives the ratio $k_p/k_t^{1/2}$ evaluated from Equation (14). Separate values of α_λ for monomer and initiator were used to evaluate the integrals. Individual values for the quantum yields are also required, since Equation (14) is based on the concept that both initiator and monomer form activated species. The experimental value $\phi_{\exp}$ should be equal to the sum of ϕ_M and ϕ_{In}. Then individual values were determined by finding the ratio ϕ_{In}/ϕ_M which gave the best agreement with the experimental rates. This ratio turned out to be approximately 500. Despite its high value, the contributions of the two terms in Equation (14) were of the same magnitude. Table 1 gives the results for $k_p/k_t^{1/2}$ obtained in this way. The variations are large and exhibit trends with concentration. Using the average value 0.088, rates were calculated from Equation (14) and are represented by the dotted lines in Figures 5 to 7. The effects of intensity and initiator concentration are reasonably well predicted, but not the 1.5 order with respect to monomer (Figure 7).

The only quantitative values found in the literature for $k_p/k_t^{1/2}$ for acrylamide polymerization are those of Suen et al. (1958) who used a batch photochemical apparatus. Employing the redox initiator and a rotating-sector method, these investigators obtained 3.9, reasonably close to the average result of 3.0 from Equation (15). This agreement is not considered significant because of the uncertainties involved in obtaining numerical results, particularly the assumptions of a radial light model, an average quantum yield ϕ independent of wave length, and the approximate value of $\phi_{\exp}$. Nevertheless, the numerical results should be useful for designing photoreactors for this polymerization when the same lamp-reactor geometry and same type of lamp are used.

In summary, our data show better agreement with an empirical rate equation, based upon only activated initiator molecules initiating polymerization, than with an expression which supposes that both activated monomer and initiator molecules can cause polymerization. Accepting this, the effect of monomer concentration on the induction period and the 1.5 order must be ascribed to some interaction between activated initiator molecules and monomer, such as the cage effect, complex formation, etc.

ACKNOWLEDGMENT

The financial assistance of the National Science Foundation, Grant GK-34536, is gratefully acknowledged.

NOTATION

A_λ = absorbance, $A_\lambda = \log_{10}(1/T_\lambda)$
C = concentration, g mole/liter
F_λ = UV energy output of lamp at wave length λ, Einsteins/s; F_t = total UV output
$[In]$ = initiator concentration, g moles/liter
$I_{r,\lambda}$ = local intensity at radius r of annular reactor and for wave length λ, Einsteins/(cm^2)(s)
$I_{w,\lambda}$ = intensity at wall of reactor ($r - \eta R$), Einsteins/(cm^2) (s)
$I_{b,t}$ = total intensity for polychromatic radiation at reactor wall without filter solution, Einsteins/(cm^2) (s)
k_i = rate constant for initiation steps, s^{-1}
k_p = rate constant for propagation steps, cm^3/(g mole) (s)
k_t = rate constant for termination steps, cm^3/(g mole) (s)
$(k_p/k_t^{1/2})_E$ = ratio of rate constants in Equations (9) and (15), (liter/g mole)$^{\beta - 1/2}$(s)$^{-1/2}$
L = radiation path length, cm
$[M]$ = monomer concentration, g mole/liter
$[O_2]_0$ = initial concentration of dissolved oxygen, g mole/liter
$[Ox]$ = oxalic acid concentration, g mole/liter
Q = volumetric flow rate, cm^3/s
R = outer radius of annular reactor, cm; ηR = inner radius
r = radial coordinate, cm
T = induction period, s
T_λ = transmittance (fraction of light transmitted) at wave length λ
V_R = irradiated volume of reactor, cm^3
V_s = total volume of solution in reactor system, cm^3
t = reaction time, s

Greek Letters

α_λ = absorptivity of wave length λ, defined by Equation (16), liter/(g mole) (cm)
β = reaction order for $[M]$ in Equation (9)
$\Omega(r)$ = polymerization rate at radius r in annular reactor, g moles/(liter)(s)
$\overline{\Omega}$ = average over reactor volume
$\overline{\Omega}_{\text{exp}}$ = experimentally determined average rate
$\overline{\Omega}_{Ox}$ = average rate of reduction of oxalic acid
$\overline{\Omega}_{In}$ = average rate of initiation step
ϕ = quantum yield, g mole/Einstein
ϕ_{exp} = quantum yield for initiation step, as measured experimentally
ϕ_{In} = quantum yield for the activation of initiator molecules
ϕ_M = quantum yield for the activation of monomer molecules
μ = attenuation coefficient, cm^{-1}

Subscripts

In = initiator
M = monomer
Ox = oxalic acid
0 = initial or feed
p = product stream from reactor

LITERATURE CITED

Bagdasar'yan, Kh. S., *Theory of Free-Radical Polymerization*, p. 62-160, Israel Program for Sci. Transl., Jerusalem (1968).

———., "Photopolymerization of Vinyl Acetate, *Zhur. Fiz. Khim.* **18**, 294 (1944); "Kinetics of Photopolymerization in the Presence of an Inhibitor," *ibid.*, **21**, 25 (1947); "Photopolymerization of Vinyl Compounds," *ibid.*, **22**, 1181 (1948).

———., "Photopolymerization of Methyl Acrylate," *Issled. v. obl. vysokomol. soed.* 339 (1949).

Bamford, C., and M. Dewar, "Photopolymerization of Methyl Methacrylate," *Nature*, **163**, 214 (1949).

Bamford, C. H., A. D. Jenkins, and R. Johnston, "Termination Reaction in the Polymerization of Acrylonitrile," *Trans. Faraday Soc.*, **55**, 1451 (1959).

Bevington, J. C., *Radical Polymerization*, p. 1-188, Academic Press, New York (1961).

Burnett, G. M., and L. D. Loan, "High-Conversion Polymerization of Methyl Methacrylate," *Trans. Faraday Soc.*, **55**, 1451 (1959).

Calvert, J. G., and J. N. Pitts, "Photochemistry," p. 598, Wiley, New York (1966).

Cassano, A. E., and J. M. Smith, "Photochlorination in a Tubular Reactor," *AIChE J.*, **12**, 1124 (1966).

Chapiro, A., M. Magat, J. Sebban, and P. Wahl, "Polymerization of Styrene by x-Rays," *Ric. Sci. Suppl.*, 25A, 73 (1955).

Denbigh, K. G., "Kinetics of Steady-State Polymerization," *Trans. Faraday Soc.*, **43**, 648 (1947).

Flory, P. J., *Principles of Polymer Chemistry*, p. 95-136, Cornell Univ. Press, Ithaca, New York (1953).

Fujimoto, J., M. S. thesis, "Polymerization of Acrylamide," Kyoto Univ., Japan (1967).

Goppalan, M. R., and M. Santappa, "Polymerization of Styrene in Solution," *Makromol. Chem.*, **50**, 83 (1963).

Hamm, G. E., *Vinyl Polymerization*, Vol. I, Part I, Marcell Dekker, New York (1967).

Huyser, E. S. *Free Radical Chain Reactions*, p. 76-150, Interscience, New York (1970).

Jain, R. L., W. W. Graessley, and J. S. Dranoff, "Design and Analysis of a Photoreactor for Styrene Polymerization," paper presented at the Third Joint Meeting AIChE and Puerto Rican Inst. Chem. Eng., San Juan (1970).

Jenkins, A. D., "Retardation in Vinyl Polymerization," *Trans. Faraday Soc.*, **54**, 1885 (1958).

Kamenskaya, S., and M. Medvedev., "Kinetics of the Polymerization of Vinyl Acetate," *Acta Physiocochim. USSR*, **13**, 565 (1940).

Mark, H. F., and D. Josefowitz, "Vinyl Polymerization in Solution," *Polymer Bull.*, **1**, 140 (1945).

Mark, H. F., and R. Raff, *High Polymeric Reactions: Their Theory and Practice*, p. 36-72, Interscience, New York (1961).

Matheson, M. S., "Chain Initiation in Catalyzed Polymerization," *J. Chem. Phys.*, **13**, 584 (1945).

Marvel, C. S., and C. L. Levesque, "The Structure of Vinyl Polymers. VII. Polyacrylyl Chloride," *J. Am. Chem. Soc.*, **61**, 3244 (1939).

Marvel, C. S., and E. H. Riddle, "The Structure of Vinyl Polymers. IX. Catalysts," ibid., **62**, 2666 (1940).

Newkirk, A. E., "The Preparation and Polymerization of Vinyl Fluoride," *ibid.*, **68**, 2467 (1946).

Noyes, R. M., "Kinetics of Competitive Processes when Reactive Fragments are Produced in Pairs," *ibid.*, **77**, 2042 (1955).

Schulz, G. V., and E. Husemann, "Kinetics of Polymerization Processes," *Z. Physik. Chem., Leipzig*, **B39**, 246 (1938).

Suen, Tzeng-Jiueq, Y. Yen, and J. V. Lockwood, "Polymerization of Acrylamide with Chlorate-Sulfite Initiator," *J. Polymer Sci.*, **31**. 481 (1958).

Taylor, G. B., and H. W. Starkweather, "Kinetics of Polymerization of Vinyl Acetate," *J. Am. Chem. Soc.*, **52**, 4708 (1930).

Tudos, Ferenc, "Kinetics of Radical Polymerization," *Makromol. Chem.*, **79**, 8 (1964).

———., "Kinetics of Inhibition of Radical Polymerization," *Acta Chim. Hung.*, **43**, 397 (1965).

Manuscript received August 21, 1972; revision received December 27, 1972, and accepted January 12, 1973.